

Thermal and Magnetoelastic Properties of the van der Waals Ferromagnet $\text{Fe}_{3-\delta}\text{GeTe}_2$: Anisotropic Spontaneous Magnetostriction and Ferromagnetic Magnon Excitations

Reinhard K. Kremer^{1,*} and Eva Brücher^{1,†}

¹Max Planck Institute for Solid State Research, Heisenbergstrasse 1, D-70569 Stuttgart, Germany

(Dated: January 26, 2024)

By determining the lattice parameters as a function of temperature of the hexagonal van der Waals ferromagnet $\text{Fe}_{2.92(1)}\text{Ge}_{1.02(3)}\text{Te}_2$ we obtain the temperature dependence of the spontaneous in-plane magnetostriction in the ferromagnetic and the linear thermal expansion coefficients in the paramagnetic state. The spontaneous magnetostriction is clearly seen in the temperature dependence of the in-plane lattice parameter $a(T)$, but less well pronounced perpendicular to the planes along c . Below T_C the spontaneous magnetostriction follows the square of the magnetization and leads to an expansion of the hexagonal layers. Extrapolating to $T \rightarrow 0$ K we obtain a spontaneous in-plane saturation magnetostriction of $\lambda_{\text{sp},a}(T \rightarrow 0) \approx -220 \times 10^{-6}$. In the paramagnetic state the linear thermal expansion coefficients amount to $13.9(1) \times 10^{-6} \text{ K}^{-1}$ and to $23.2(2) \times 10^{-6} \text{ K}^{-1}$ for the in-plane and out-of-plane direction, respectively, indicating a linear volume thermal expansion coefficient of $50.8(4) \times 10^{-6} \text{ K}^{-1}$ which we use to estimate the volume thermal expansion contribution to the heat capacity determined at constant pressure. A Sommerfeld-type linear term in the low-temperature heat capacities can be quantitatively ascribed to 2dim ferromagnetic magnon excitations.

INTRODUCTION

Two-dimensional (2dim) van der Waals (vdW) ferromagnets with sufficiently high Curie temperatures lately have attracted special attention with respect to their applicability in modern nanoelectronic and spintronic devices. Among a number of prominent systems, the ternary iron germanium telluride, $\text{Fe}_{3-\delta}\text{GeTe}_2$ ($\delta \approx 0.1$) (FGT), with a Curie temperature, T_C , close to 220 K has been intensively investigated. After the initial synthesis of polycrystalline specimen and the basic structural and magnetic characterization,^[1] accessibility of larger crystalline samples enabled a broad variety of experiments with a focus on mono- and multilayer samples. These proved FGT to be a highly promising platform for studying the complex interplay of magnetic and electronic properties in reduced dimensions up to the point of monolayer devices.

FGT exhibits a number of intriguing magneto-electronic properties: Below T_C FGT is an itinerant ferromagnet.^[1, 2] Though, an antiferromagnetic transition at ~ 150 K has also been conjectured.^[3] Using density functional calculations Jang *et al.* concluded that Fe defects and hole doping are the key to drive FGT into the ferromagnetic phase, whereas they proposed that stoichiometric FGT to be antiferromagnetic.^[4]

A large anomalous Hall effect already at small polarizing external magnetic fields has been found for bulk samples.^[5–8] Exfoliated monolayers still show uniaxial anisotropy and robust ferromagnetism, however with T_C reduced to ~ 130 K.^[9, 10] Broadest interest attracted the electrolyte gating experiments by Deng *et al.*. They showed that already small gate voltages applied to flakes of FGT with Li^+ intercalated in between the Te double layers can tune T_C from 100 K up to room

temperature.^[11] Laser-induced spin and charge photocurrents in single-layer FGT were predicted by first-principles calculations suggesting applications of FGT in opto-spintronics.^[12] Néel- or Bloch-type skyrmions have been reported to occur in FGT monolayers.^[13–17] Xu *et al.* argued that unusual terms in the Hamiltonian connecting four spins can account for these observations.^[18] Recently, successful generation and manipulation of terahertz spin-current has been reported by Chen *et al.*^[19]

Despite the booming interest in the magnetic and magnetoelectric properties of FGT, the lattice properties and especially magnetoelastic coupling still remained scarcely explored. By using density-functional theory Zhuang *et al.* found that the orbital moment of the Fe atoms is sizeable, causing a large magnetic anisotropy energy increasing with tensile strain, and a large in-plane magnetostrictive coefficient of -559×10^{-6} for monolayer FGT.^[9] In Raman spectroscopy measurements Milosavljević *et al.* observed fingerprints of spin-phonon coupling at around 152 K and also anomalous behavior of the Raman frequencies and mode linewidths at the ferromagnetic transition.^[20]

FGT crystallizes in the hexagonal crystal system with lattice parameters $a \approx 3.99 \text{ \AA}$ and $c \approx 16.34 \text{ \AA}$. The crystal structure of FGT contains slabs of Fe_3Ge sandwiched by vdW bonded Te double layers.^[1] The Fe atoms occupy two different crystallographic sites. Notably, the Fe2 site (Wyckoff position 2c) in samples prepared under stoichiometric conditions is not fully occupied (typically $\delta \sim 0.1$), whereas the Fe1 site, within error bars, exhibits no deficiency. Increasing δ , i.e. enlarging the Fe2 deficiency reduces T_C . The in-plane lattice parameter a decreases with increasing δ , whereas the out-of-plane lattice parameter c increases for larger Fe2 deficiency.^[21] Strong uniaxial anisotropy aligns the Fe magnetic moments along the

c easy axis making FGT an auspicious platform for magnetic data storage devices.[9, 22–24] The ordered magnetic moments of the Fe atoms for $\delta = 0.1$ amount to $2.2 \mu_B$ for the Fe1 and $1.5 \mu_B$ for the Fe2 crystallographic sites, respectively.[21] For $\delta \sim 0.25$ both ordered moments converge to a common value of $\sim 1.4 \mu_B$.[9, 21]

Here, we report on measurements of the zero-field spontaneous magnetostriction when FGT enters into the ferromagnetic state. Magnetostriction, i.e. the deformation of the geometrical shape of a ferromagnetic specimen during the magnetization process can be evoked e.g. by an external magnetic field. Especially magnetic field induced magnetostriction is of great technological importance but also fundamental to model the magnetization process itself and the formation of the domain structure. Magnetostriction induced by an external magnetic field depends on the orientation of the external magnetic field with respect to the orientation of domain magnetization and the direction of the exchange interaction between the magnetic moments.[25] Spontaneous magnetostriction where the shape change, $\lambda = \delta l(T)/l(T)$, is initiated by the increase of the spontaneous magnetization $M(T < T_c, H = 0)$ below T_C in vanishing external magnetic field H i.e. by the internal ferromagnetic domain formation can provide very valuable information, e.g. about spontaneous reorientation processes and changes in the domain structure. Technologically magnetostrictive effects may become important for the interaction of FGT monolayers deposited on substrates.

In addition, we review preceding heat capacity experiments which have found large linear terms in the low and high temperature specific heats which the authors attributed to magnetic contributions.[2] Especially in the paramagnetic regime, the published heat capacity data substantially overshoot the Dulong-Petit limit, suggesting a critical reconsideration of the thermal properties. By using the linear thermal volume expansion coefficients in the paramagnetic state to determine the lattice expansion contribution to the heat capacities measured at constant pressure, C_p , we revise these findings.

The Sommerfeld-like linear term in the low-temperature heat capacities can be quantitatively attributed to 2dim ferromagnetic magnon excitations. A comparison with the spin stiffness constants found by inelastic neutron scattering gives quantitative agreement.

EXPERIMENTAL

Samples of FGT were prepared from stoichiometric mixtures of powders of the elements, Fe (Alfa Aesar, purity 99.998%), Ge (Thermo Fisher, purity 99.999%) and Te (Thermo Fisher, purity 99.999%) using a minute amount of iodine as mineralizer. The starting materials were thoroughly mixed and reacted in evacuated quartz glass tubes in a two-zone furnace heated to temperatures

between 750°C and 650°C. Phase purity and composition of the samples was checked by energy-dispersive spectroscopy (EDX) employing a Tescan Vega4 LMU SEM equipped with an Oxford X-Max^NN20 detector and by x-ray powder diffraction (XRPD) using $\text{MoK}\alpha_1$ and $\text{CuK}\alpha_1$ radiation. The magnetic properties of the sample were determined by powder and single crystal dc magnetization (MPMS, Quantum Design) and specific heat measurements (PPMS, Quantum Design).

The lattice parameters of a polycrystalline sample of FGT were determined in zero external magnetic field as a function of temperature from Rietveld profile analysis[26] of XRPD patterns collected on a Bruker D8 Discovery x-ray diffractometer (Bragg-Brentano scattering geometry) using $\text{CuK}\alpha_1$ radiation. A PHENIX (Oxford Cryosystems) closed cycle cooling cryostat was used to set the temperature of the sample. Each XRPD pattern was collected at stabilized temperature. The particle size of the powder was adjusted to $63 \mu\text{m}$ or less by straining the powder through sieves of the respective mesh size. The powder sample was thermally anchored with ApiezonN vacuum grease to the sample holder platform, equipped with an inlay of a Si wafer specially oriented to suppress background scattering from the sample holder.

RESULTS AND DISCUSSION

Sample Characterization

Figure 1 displays a SEM picture of a typical crystal analyzed with energy dispersive x-ray spectroscopy. Three spots on an a - b surface were tested and very good agreement was found for the element concentration, proving homogeneity of the element concentration. EDX analyses carried out on crystals of several other FGT sample preparations indicated a spread of the Fe2 concentration of $0.82 \leq (1 - \delta) \leq 0.92$.

XRPD on crushed crystals and polycrystalline samples of FGT proved phase purity of our specimen. Figure 2 displays a typical room-temperature XRPD pattern analyzed with a Rietveld profile refinement assuming the structure model proposed by Deiseroth *et al.* (space group $P6_3/mmc$, no. 194).[1] At room temperature the refined lattice parameters amount to $a = 3.99939(8) \text{ \AA}$ and $c = 16.3225(4) \text{ \AA}$, in good agreement with the values reported by Deiseroth *et al.*. In the refinements the Ge and Fe1 lattice sites were assumed to be fully occupied, whereas for Fe2 the occupancy converged to 0.918(11), in good accord with the EDX result. At room temperature the z -positional parameter of the Te and Fe1 atoms (Wyckoff positions 4f and 4e, respectively) were refined to 0.5902(2) and 0.6702(3), also in good agreement with the values obtained from single crystal structure determination.[1]

The Curie temperatures of the FGT samples were de-

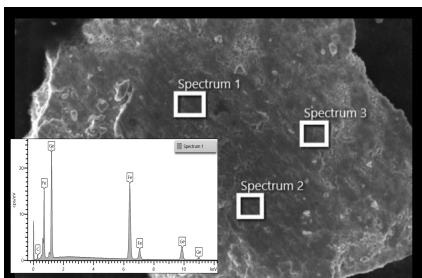


FIG. 1. SEM image of a crystal of our sample with the rectangles marking the areas where EDX element analysis was performed. The variation of element concentration across the analyzed areas amounted to less than 0.5%, 1.4% and 0.07% for Fe, Ge and Te, respectively. The lower inset shows the SEM spectrum collected at spot no. 1.

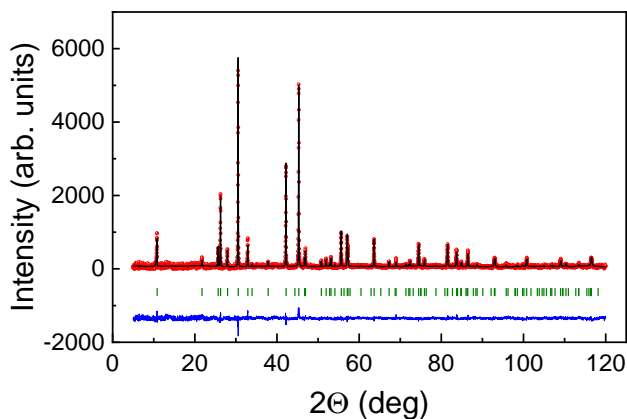


FIG. 2. (color online) XRD pattern of FGT ($\text{CuK}\alpha_1$ radiation) collected at 295 K. The red circles represent the experimental data, the solid black line show the result of the Rietveld profile refinement and the vertical green bars mark the positions of the Bragg reflections used to calculate the refined pattern.

terminated from heat capacity and magnetization measurements. Figure 3 summarizes the magnetic susceptibilities and the specific heat of the sample with composition $\text{Fe}_{2.92(1)}\text{Ge}_{1.00(3)}\text{Te}_2$. The magnetization data exhibit the characteristic splitting of the zero-field cooled (zfc) and field - cooled (fc) branches reported before.[1] The zfc - fc hysteresis closes with increasing magnetic field. The steepest descent of the magnetization is found at ~ 218 K (see inset (b) in Figure 3) where also the λ -type anomaly in the specific heat is observed (Figure 3(d)). At room temperature the heat capacity linearly approaches a value of ~ 156 J/molK, consistent with the Dulong-Petit value of $5.92 \times 3R$, where R is the molar gas constant, but substantially lower than the findings reported by Bin Chen *et al.*[2] The linear increase of the heat capacity will be discussed in detail below. At low temperatures in the ferromagnetic state the heat capac-

ities follow a power law (Figure 3(e))

$$C_{\text{mol}}/T = \gamma + \beta T^2, \quad (1)$$

with $\gamma = 109(1)$ mJ/molK², close to what has been observed by Bin Chen *et al.*[2] The slope $\beta = 1.25(6)$ mJ/molK⁴ implies a Debye temperature, $\Theta_{\text{Deb}}(T \rightarrow 0 \text{ K})$ of 210(2) K. The majority of the linear contribution to the heat capacity can be ascribed to two-dimensional ferromagnetic magnons, as will be analyzed in detail below.

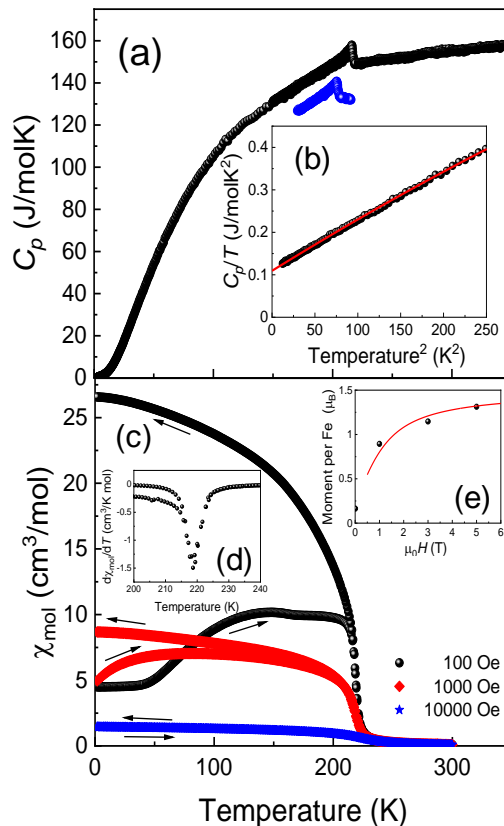


FIG. 3. (color online) (upper panel, black circles) (a) Molar heat capacity of a crystal of $\text{Fe}_{2.92(1)}\text{Ge}_{1.02(3)}\text{Te}_2$. The blue dots exemplify the reduction of the Curie temperature for a sample with element composition $\text{Fe}_{2.85}\text{GeTe}_2$ (data down-shifted by 10 J/molK for better comparison). (b) displays the power law behavior at low temperatures. (lower panel) (c) zfc and fc magnetic susceptibilities (indicated by the arrows) of the FGT sample of composition $\text{Fe}_{2.92(1)}\text{Ge}_{1.02(3)}\text{Te}_2$ measured with external magnetic fields of 100 Oe, 1 kOe and 10 kOe. The inset (d) displays the derivative of the magnetization measured with an external field of 100 Oe as a function of temperature. The (upper) inset (e) shows the magnetic moment per Fe atom. The (red) solid line is a guide to the eye.

The Curie temperature T_C depends on the Fe2 content. An increase of δ leads to a reduction of the Curie temperature (see blue dots in Figure 3(a)). Figure 4(a)

displays the variation of the Curie temperature as a function of the composition around $\delta \approx 0.1$. A decrease of T_C is paralleled by a decrease of the volume of the crystallographic unit cell (Fig. 4(b)), the latter induced by the decrease of the in-plane lattice parameter a .

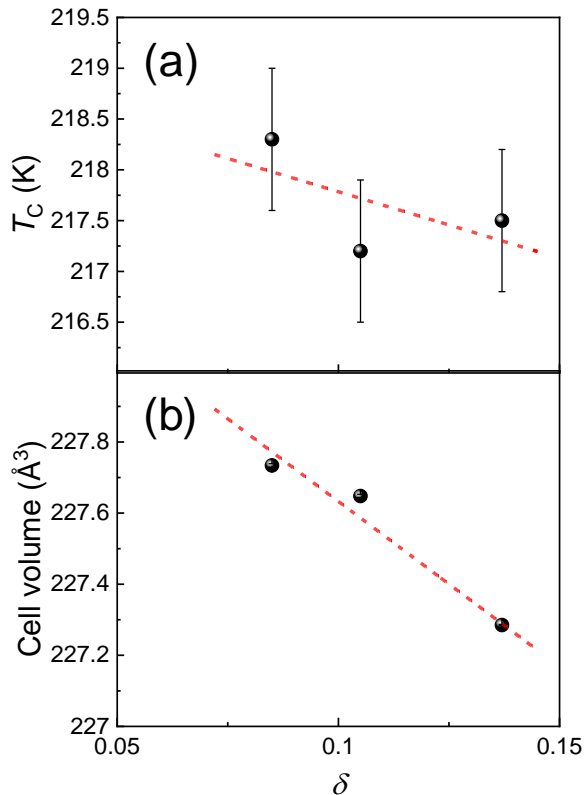


FIG. 4. (color online) (a) Curie temperature, T_C as a function of the Fe2 deficiency, δ of our samples. δ was determined from the Rietveld refinements of the XRPD patterns collected using $\text{MoK}\alpha_1$ radiation and from EDX analyses. (b) Volume of the crystallographic unit cell as a function of δ . The (red) dashed lines are guides to the eye.

Spontaneous Magnetostriction

A fraction of the same sample with composition $\text{Fe}_{2.92(1)}\text{Ge}_{1.02(3)}\text{Te}_2$ which had never been exposed to an external field was subsequently used for the temperature dependent XRPD measurements. Figure 5 displays the reduced lattice parameters $a^*(T)=a(T)/a(295\text{ K})$ and $c^*(T)=c(T)/c(295\text{ K})$, relative to their room temperature values, as derived from the Rietveld profile refinements of the temperature dependent XRPD patterns. With decreasing temperature the relative contraction of the lattice parameters perpendicular to the layers is about a factor of two larger than the in-plane contraction. In the paramagnetic regime the cell volume and the lattice parameters decrease linearly with temperature with

rates $(dV_{\text{cell}}/dT)/V_{\text{cell}}(295\text{ K}) = -50.8(4)\times 10^{-6}\text{ K}^{-1}$, and $-13.9(2)\times 10^{-6}\text{ K}^{-1}$, and $-23.2(2)\times 10^{-6}\text{ K}^{-1}$, for a and c , respectively.

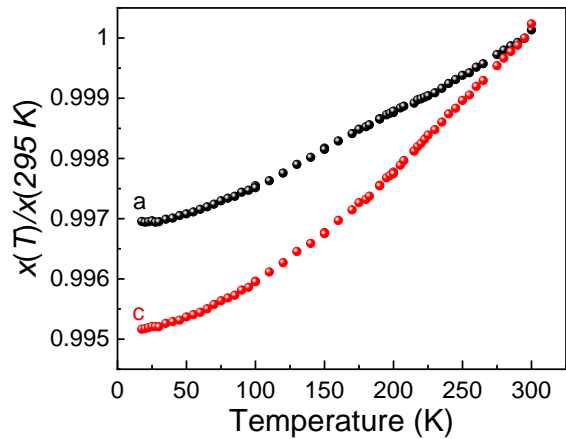


FIG. 5. (color online) Temperature dependence of the lattice parameters $a^*(T)=a(T)/a(295\text{ K})$ and of $c^*(T)=c(T)/(295\text{ K})$.

Figure 6 displays the temperature dependence of the z -positional parameters of the Te and the Fe1 atoms. Whereas $z(\text{Fe1})$ shows a faint increase with decreasing temperature, still within error bars, the z positional parameter of the Te atoms decreases and levels off at low temperatures.

Figure 7 compiles the volume of the hexagonal unit cell and the lattice parameters $a(T)$ and $c(T)$ as a function of the temperature. Whereas the in-plane lattice parameter $a(T)$ exhibits a noticeable shoulder near $T \sim T_C$, $c(T)$ bends away from the high-temperature linear behavior before leveling off at low temperatures. A noticeable response to the onset of ferromagnetic order is not seen for the out-of-plane lattice parameter c . The shoulder in $a(T)$ is ascribed to a negative spontaneous in-plane magnetostriction, i.e. an expansion of the hexagonal planes, induced by ferromagnetic ordering.

Extrapolating the linear behavior of $a(T)$ from the paramagnetic regime and subtracting from the data below T_C , reveals a spontaneous in-plane magnetostriction starting below $\sim 223\text{ K}$, which saturates below $\sim 50\text{ K}$. The temperature dependence of the spontaneous magnetostriction (see Figure 8) is reminiscent of a continuous phase transition with a critical temperature of $223(1)\text{ K}$, matching T_C , as determined from the magnetization and specific heat experiments. A tentative extrapolation of the spontaneous magnetostriction to $T \rightarrow 0\text{ K}$ (see the black dashed line in Fig. 8) indicates a spontaneous in-plane saturation magnetostriction, $\lambda_{\text{sp},a}(0)$, of

$$\lambda_{\text{sp},a}(T \rightarrow 0) \approx -2.2 \times 10^{-4}.$$

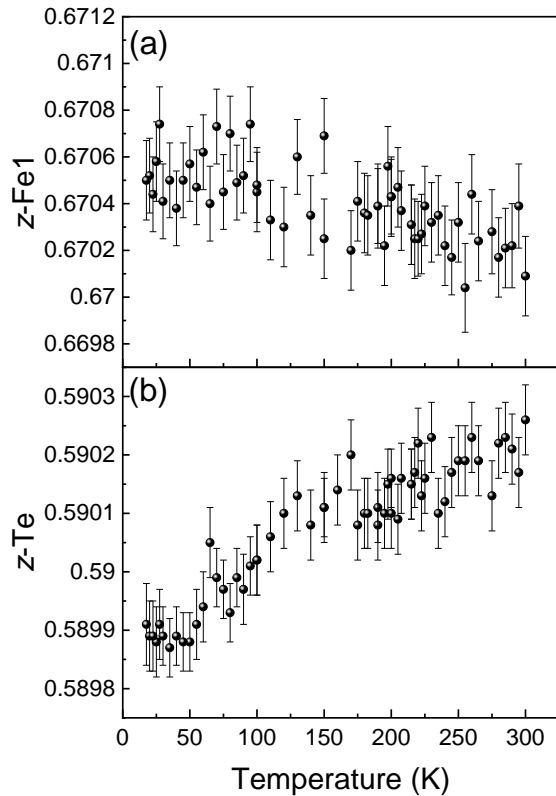


FIG. 6. z positional parameters of the (a) Fe1 and (b) the Te atoms (Wyckoff positions 4e and 4f, respectively) of $\text{Fe}_{2.92(1)}\text{Ge}_{1.02(3)}\text{Te}_2$ as a function of temperature.

Attempts to model the temperature dependence of the lattice parameters to a Debye function over the whole temperature range lead to unstable fits and were not meaningful. For the same reason the out-of-plane spontaneous magnetostriction was difficult to ascertain since there is no visible anomaly in the temperature dependence of the c -lattice parameter at T_C .

In order to relate the spontaneous magnetostriction to the temperature dependence of the magnetization we carried out isothermal magnetization measurements on a thin crystal platelet of $\text{Fe}_{2.92(1)}\text{Ge}_{1.02(3)}\text{Te}_2$ with the magnetic field aligned along the c -axis. After a correction for the demagnetizing field, we derived the temperature dependence of the zero-field magnetization from modified Arrott Belov plots [27, 28] (see inset in Fig. 9). The zero-field magnetization can be very well fitted to a critical power law (see Fig. 9) given by

$$M(T) = M_0(1 - T/T_C)^\beta, \quad (2)$$

with a critical exponent $\beta = 0.32(1)$, consistent with findings reported earlier by Liu et al. [29, 30]

Fig. 10 displays the temperature dependence of the spontaneous magnetostriction as a function of the magnetization. The log-log plot reveals a power law behavior

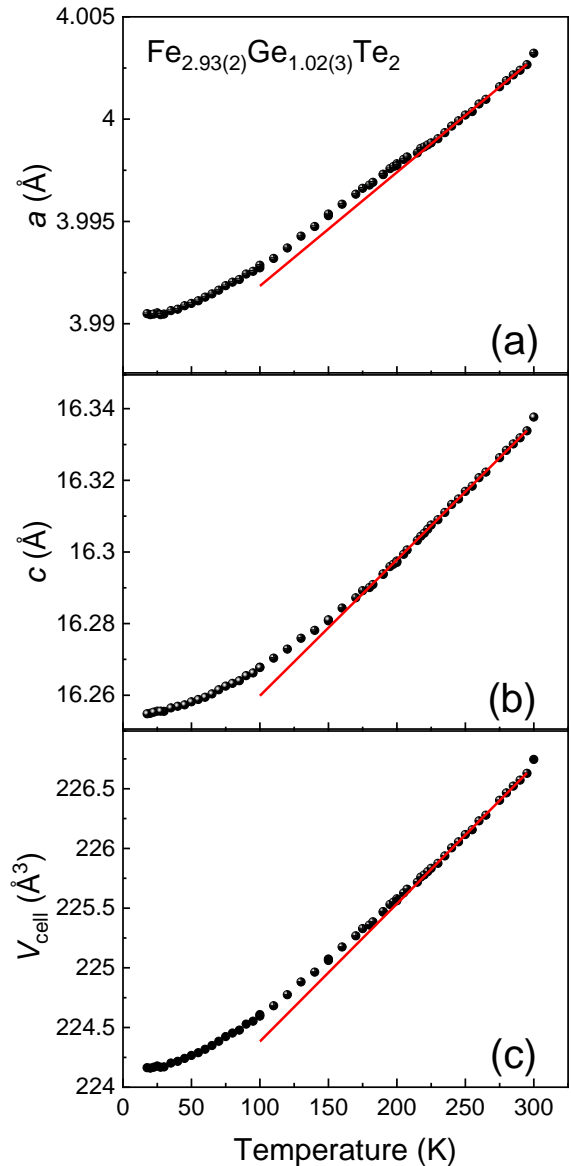


FIG. 7. (color online) Temperature dependence of the lattice parameters a (a), c (b), and the cell volume (c) of $\text{Fe}_{2.92(1)}\text{Ge}_{1.02(3)}\text{Te}_2$. Error bars are of the size of the symbols. The solid (red) lines represent linear fits between 235 K and 295 K of the temperature dependence of the respective quantities. The relative slopes are given in the text.

of the spontaneous magnetostriction according to

$$\lambda_{\text{sp},a}(T) = [M_0(1 - T/T_C)^\beta]^{1.5(1)}. \quad (3)$$

Taking into consideration the critical exponent $\beta = 0.32$ for the magnetization, eq.(3) indicates a critical exponent for the spontaneous in-plane magnetostriction of ~ 0.48 , i.e. close to the critical exponent expected for mean field behavior.

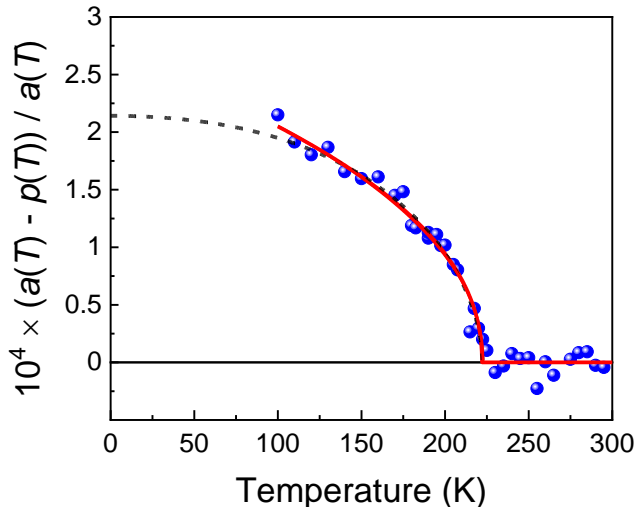


FIG. 8. (color online) Spontaneous in-plane magnetostriction of $\text{Fe}_{2.92(1)}\text{Ge}_{1.02(3)}\text{Te}_2$ as a function of temperature. The red solid line is a fit to a critical power law, τ^β with the reduced temperature $\tau = 1 - (T/T_C)$ with a critical temperature, T_C 222.4(8) K and a critical exponent $\beta = 0.48(2)$. The black dashed line represents an extrapolation to $T \rightarrow 0$ K.

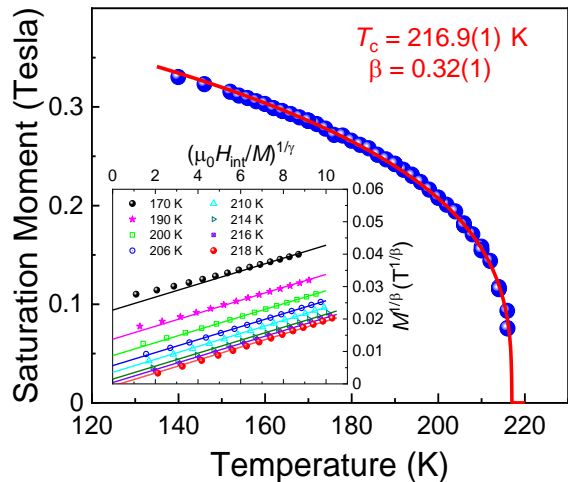


FIG. 9. (color online) Temperature dependence of the zero-field spontaneous magnetization of $\text{Fe}_{2.92(1)}\text{Ge}_{1.02(3)}\text{Te}_2$ derived from modified Arrott-Nowotny plots displayed (lower inset) adopting critical exponents $\beta = 0.33$ and $\gamma = 1.38$. The main frame shows a fit of the magnetization with a power-law temperature dependence (solid red) line according to eq. (2).

Thermal Lattice Expansion Contribution to the Specific Heat

In a first investigation of the heat capacities of FGT Bin Chen *et al.* had found large linear contributions at low and high temperatures, hitherto no conclusively

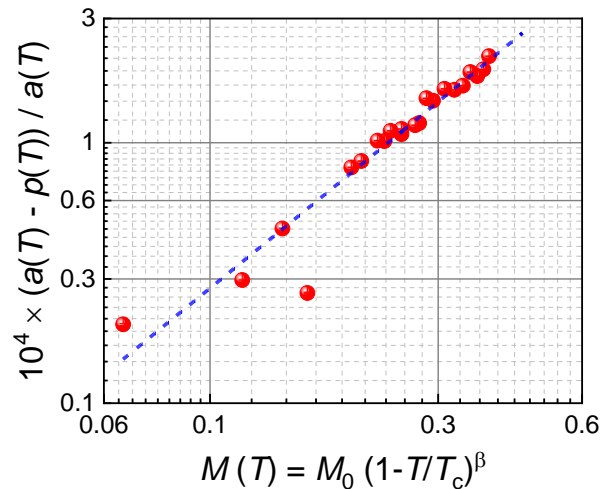


FIG. 10. (color online) Log-log plot of the spontaneous in-plane magnetostriction as a function of the magnetization. The blue dashed line corresponds to a power law with an exponent 1.5.

explained.[2] At room temperature they found a value of ~ 200 J/molK and a stark linear increase above T_C , which they attributed to electronic and magnetic contributions.[2]

In contrast to these earlier findings our heat capacity data measured at constant pressure, C_p , (see Fig. 3(d)) tend to a value of ~ 156 J/molK, only moderately exceeding the Dulong-Petit limit for the heat capacity at constant volume, $C_v(T \rightarrow \infty) \times 3NR = 148$ J/molK, with $N = 5.92$ being the number of atoms per formula unit and R the molar gas constant. At 350 K our C_p data attain a value of ~ 158 J/molK, substantially lower than that reported by Bin Chen *et al.*

In the following, using our thermal expansion data for $T > T_C$, we estimate the electronic and the lattice thermal expansion contribution to the heat capacities at high temperatures. The difference between the heat capacities measured at constant pressure and at constant volume is given by

$$C_p - C_v = \alpha_v^2(T) B V_{mol} T, \quad (4)$$

where $\alpha_v(T)$ is the temperature dependent coefficient of the volume thermal expansion, B is the bulk modulus and V_{mol} the molar volume.

In the paramagnetic regime above T_C and up to room temperature the lattice expands approximately linearly with increasing temperature. The linear thermal expansion coefficients amount to $\alpha_a = 13.9(1) \times 10^{-6} \text{ K}^{-1}$ and to $\alpha_c = 23.2(2) \times 10^{-6} \text{ K}^{-1}$ for the in-plane and out-of-plane direction, respectively, resulting in a linear volume thermal expansion coefficient of $\alpha_v = 50.8(4) \times 10^{-6}$. The in-plane linear thermal expansion coefficient of $\text{Fe}_{2.92(1)}\text{Ge}_{1.02(3)}\text{Te}_2$ in the paramagnetic state compares

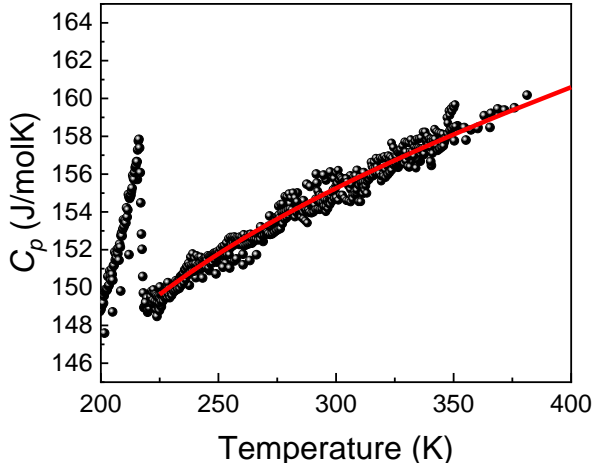


FIG. 11. (color online) High-temperature heat capacities at constant pressure, C_p , of $\text{Fe}_{2.92(1)}\text{Ge}_{1.02(3)}\text{Te}_2$. The solid (red) line is a fit to eq.(5) with parameters given in the text.

well with that of elementary iron for which an expansion coefficient of 11.6×10^{-6} was observed at room temperature.[31]

In order to fit the heat capacity at high temperatures displayed in Figure 11 we used a series expansion for the Debye contribution[32] and included a term linear in temperature, $E T$,

$$C_p(T) = 5.92 \times 3 R \left(1 - \frac{1}{20} \frac{\Theta_\infty^2}{T^2} + \frac{1}{560} \frac{\Theta_\infty^4}{T^4}\right) + E T, \quad (5)$$

with R being the gas constant, and Θ_∞ the Debye temperature. $E T$ comprises the thermal expansion contribution given by Eq. (4) but also a linear electronic (Sommerfeld) term γ . A fit of the heat capacities of several runs (Fig. 11) using data for $T > 225$ K yields

$$E = 37(2) \text{ mJ/molK}^2,$$

and

$$\Theta_\infty = 222(3) \text{ K},$$

the latter being very close to the Debye temperature $\Theta_{\text{Debye}}(T \rightarrow 0 \text{ K})$ which amounts to 210 K.

The Sommerfeld-term, γ , from the heat capacity of the conduction electrons can be estimated from

$$\gamma = \frac{\pi^2 k_B^2}{3} N(E_F), \quad (6)$$

with the Boltzmann constant k_B and the electronic density of states $N(E_F)$ at the Fermi level. The electronic densities of states for two spin directions at E_F per formula unit obtained from density functional calculations has been reported to 6(2) states/eV.[33, 34] Using this

value and Eq. (6) one arrives at a conduction electron term of 14 mJ/molK² and at a value of 23 mJ/molK² for the thermal expansion contribution. Adopting the volume thermal expansion coefficient $\alpha_{\text{Vol}} = 50.8 \times 10^{-6} \text{ K}^{-1}$ and the molar volume $V_{\text{mol}} = 6.785 \times 10^{-5} \text{ m}^3\text{mol}^{-1}$ [1] results in a Bulk modulus B of

$$B \sim 130(40) \text{ GPa},$$

wherein the sizeable error bar arises from the uncertainty of the electronic density of states at the Fermi energy. Our finding for the bulk modulus is by a factor of two larger than the value of ~ 70 GPa reported in literature[34, 35] The difference between our value and the reported results might be partially due to the negligence of possible electron-phonon enhancement of the electronic Sommerfeld term. We also note that for their high-pressure Mössbauer measurements O'Hara *et al.* used FGT samples with a T_C of 155 K, indicating a substantial deficit on the Fe2 site which may also affect their value for the bulk modulus.[35]

Even accepting the full value of $E \approx 37 \text{ mJ/molK}^2$ as due to the electron contribution, the excess heat capacity of almost 50 J/molK at room temperature over the Dulong-Petit limit reported by Bin Chen *et al.*[2] is far too large to be reconciled with our findings.

2dim Ferromagnetic Magnon Heat Capacity

We finally comment on the linear contribution to the low temperature heat capacity which amounts to $\sim 109 \text{ mJ/molK}^2$, again too large to be attributed to the conduction electron contribution. However, the increase *linear* in temperature, also reported by Bin Chen *et al.* with a similar magnitude, can be readily reconciled if we take ferromagnetic magnon excitations in a 2dim lattice into account. Adopting a quadratic dispersion for long-wavelength magnons in a 2dim ferromagnet the magnon contribution to the heat capacity at low temperatures varies linearly with temperature.[36] From inelastic neutron scattering data, Song Bao *et al.* have derived spin wave stiffness constants for FGT between 57 and 69 meVÅ² for the in-plane spin waves.[37] For the magnon heat capacity, C_{mag} , of a 2dim honeycomb lattice, Grosu *et al.* arrived at[38]

$$C_{\text{mag}} = R \frac{3\sqrt{3} \pi^2 a^2}{24D} T, \quad (7)$$

where R is the molar gas constant, $a \approx 4\text{Å}$ the in-plane lattice parameter and D the spin wave stiffness constant. With $D \approx 63 \text{ meVÅ}^2$ one estimates a magnon contribution linear in temperature of

$$C_{\text{mag}}/T = 123 \text{ mJ/molK}^2.$$

Adding the conduction electron contribution of $\sim 14 \text{ mJ/molK}^2$, this finding is in fair agreement

with our experimental observation of 109 mJ/molK² found from the Sommerfeld plot at low temperatures (see Fig. 3).

SUMMARY AND CONCLUSION

Using temperature dependent XRPD measurements we have determined the hexagonal lattice parameters of the 2dim van der Waals ferromagnet Fe_{2.92(1)}Ge_{1.02(3)}Te₂ which exhibits a Curie temperature of ~ 217 K. Spontaneous magnetostriction induced by the transition into the ferromagnetic state leads to an expansion of the vdW coupled layers, whereas a noticeable effect of the spontaneous magnetostriction perpendicular to the layers is not seen in the *c*-lattice parameters. For $T \rightarrow 0$ K, the in-plane spontaneous magnetostriction can be extrapolated to $\sim -220 \times 10^{-6}$ K⁻¹ by more than a factor of two smaller than the *ab-initio* calculations Zhuang *et al.*

Using the linear volume thermal expansion coefficient in the paramagnetic regime we estimate the difference of the specific heats determined at constant pressure and constant volume. The majority of the linear Sommerfeld-type contribution to the low-temperature heat capacity can be quantitatively ascribed to 2dim ferromagnetic magnon excitations.

In summary, our experimental results evidence a substantial in-plane magnetostriction for a sample of FGT with composition Fe_{2.92(1)}Ge_{1.02(3)}Te₂ having a Curie temperature of 217 K. A careful reconsideration of the heat capacities of such sample enables us to correct and understand previously reported linear contributions to the low- and high-temperature heat capacity data of FGT. Particularly noteworthy is the low-temperature magnon heat capacity contribution, linear in temperature, which can be quantitatively attributed to the layered ferromagnetic character of FGT.

Acknowledgments We thank V. Duppel for performing the SEM/EDS measurements and Hj. Deiseroth for valuable suggestions as to the preparation of FGT. A useful communication with Houlong L. Zhuang is gratefully acknowledged.

* R.Kremer@fkf.mpg.de

† E.Bruecher@fkf.mpg.de

- [1] H.-J. Deiseroth, K. Aleksandrov, C. Reiner, L. Kienle, and R. K. Kremer, Fe₃GeTe₂ and Ni₃GeTe₂ – two new layered transition-metal compounds: Crystal structures, hrtem investigations, and magnetic and electrical properties, *Eur. J. Inorg. Chem.* **2006**, 1561 (2006).
- [2] B. Chen, J. Yang, H. Wang, M. Imai, H. Ohta, C. Michioka, K. Yoshimura, and M. Fang, Magnetic properties of layered itinerant electron ferromagnet Fe₃GeTe₂, *J. Phys. Soc. Jpn.* **82**, 124711 (2013), <https://doi.org/10.7566/JPSJ.82.124711>.
- [3] J. Yi, H. Zhuang, Q. Zou, Z. Wu, G. Cao, S. Tang, S. A. Calder, P. R. C. Kent, D. Mandrus, and Z. Gai, Competing antiferromagnetism in a quasi-2d itinerant ferromagnet: Fe₃GeTe₂, *2D Materials* **4**, 10.1088/2053-1583/4/1/011005 (2017).
- [4] S. W. Jang, H. Yoon, M. Y. Jeong, S. Ryee, H.-S. Kim, and M. J. Han, Origin of ferromagnetism and the effect of doping on Fe₃GeTe₂, *Nanoscale* **12**, 13501 (2020).
- [5] C. Tan, J. Lee, S.-G. Jung, T. Park, S. Albarakati, J. Partridge, M. R. Field, D. G. McCulloch, L. Wang, and C. Lee, Hard magnetic properties in nanoflake van der waals Fe₃GeTe₂, *Nat. Commun.* **9**, 10.1038/s41467-018-04018-w (2018).
- [6] Z. Wang, D. Sapkota, T. Taniguchi, K. Watanabe, D. Mandrus, and A. F. Morpurgo, Tunneling spin valves based on Fe₃GeTe₂/hbn/Fe₃GeTe₂ van der Waals heterostructures, *Nano Letters* **18**, 4303 (2018).
- [7] K. Kim, J. Seo, E. Lee, K.-T. Ko, B. S. Kim, B. G. Jang, J. M. Ok, J. Lee, Y. J. Jo, W. Kang, J. H. Shim, C. Kim, H. W. Yeom, B. Il Min, and J. S. Yang, Bohm-Jung Kim, Large anomalous hall current induced by topological nodal lines in a ferromagnetic van der waals semimetal, *Nature Materials* **17**, 794 (2018).
- [8] Y. Liu, E. Stavitski, K. Attenkofer, and C. Petrovic, Anomalous hall effect in the van der waals bonded ferromagnet Fe_{3-x}GeTe₂, *Phys. Rev. B* **97**, 165415 (2018).
- [9] H. L. Zhuang, P. R. C. Kent, and R. G. Hennig, Strong anisotropy and magnetostriction in the two-dimensional stoner ferromagnet Fe₃GeTe₂, *Phys. Rev. B* **93**, 134407 (2016).
- [10] Z. Fei, B. Huang, P. Malinowski, W. Wang, T. Song, J. Sanchez, W. Yao, D. Xiao, X. Zhu, A. F. May, W. Wu, D. H. Cobden, J.-H. Chu, and X. Xu, Two-dimensional itinerant ferromagnetism in atomically thin Fe₃GeTe₂, *Nature Materials* **17**, 778 (2018).
- [11] Y. Deng, Y. Yu, Y. Song, J. Zhang, N. Z. Wang, Z. Sun, Y. Yi, Y. Z. Wu, S. Wu, J. Zhu, J. Wang, X. H. Chen, and Y. Zhang, Gate-tunable room-temperature ferromagnetism in two-dimensional Fe₃GeTe₂, *Nature* **563**, 94 (2018).
- [12] M. Merte, F. Freimuth, T. Adamantopoulos, D. Go, T. G. Saunderson, M. Kläui, L. Plucinski, O. Gomonay, S. Blügel, and Y. Mokrousov, Photocurrents of charge and spin in monolayer Fe₃GeTe₂, *Phys. Rev. B* **104**, L220405 (2021).
- [13] B. Ding, Z. Li, G. Xu, H. Li, Z. Hou, E. Liu, X. Xi, F. Xu, Y. Yao, and W. Wang, Observation of magnetic skyrmion bubbles in a van der waals ferromagnet Fe₃GeTe₂, *Nano Letters* **20**, 868 (2020), pMID: 31869236, <https://doi.org/10.1021/acs.nanolett.9b03453>.
- [14] M. J. Meijer, J. Lucassen, R. A. Duine, H. J. Swagten, B. Koopmans, R. Lavrijsen, and M. H. D. Guimarães, Chiral spin spirals at the surface of the van der waals ferromagnet fe3gete2, *Nano Letters* **20**, 8563 (2020), pMID: 33238096, <https://doi.org/10.1021/acs.nanolett.0c03111>.
- [15] Y. Wu, S. Zhang, J. Zhang, W. Wang, Y. L. Zhu, J. Hu, G. Yin, K. Wong, C. Fang, C. Wan, X. Han, Q. Shao, T. Taniguchi, K. Watanabe, J. Zang, Z. Mao, X. Zhang, and K. L. Wang, Néel-type skyrmion in WTe₂/Fe₃GeTe₂ van der waals heterostructure, *Nat. Commun.* **11**, 10.1038/s41467-020-17566-x (2020).
- [16] M. Yang, Q. Li, V. R. Chopdekar, R. Dhall, J. Turner, J. D. Carlström, C. Ophus, C. Klewe, P. Shafer, A. T. N'Diaye, J. W. Choi, G. Chen, Y. Z. Wu, C. Hwang,

- F. Wang, and Z. Q. Qiu, Creation of skyrmions in van der waals ferromagnet Fe_3GeTe_2 on (co/pd)(n) superlattice, *Sci. Adv.* **6**, [10.1126/sciadv.abb5157](https://doi.org/10.1126/sciadv.abb5157) (2020).
- [17] T.-E. Park, L. Peng, J. Liang, A. Hallal, F. S. Yasin, X. Zhang, K. M. Song, S. J. Kim, K. Kim, M. Weigand, G. Schütz, S. Finizio, J. Raabe, K. Garcia, J. Xia, Y. Zhou, M. Ezawa, X. Liu, J. Chang, H. C. Koo, Y. D. Kim, M. Chshiev, A. Fert, H. Yang, X. Yu, and S. Woo, Néel-type skyrmions and their current-induced motion in van der waals ferromagnet-based heterostructures, *Phys. Rev. B* **103**, 104410 (2021).
- [18] C. Xu, X. Li, P. Chen, Y. Zhang, H. Xiang, and L. Bellaiche, Assembling diverse skyrmionic phases in Fe_3GeTe_2 monolayers, *Adv. Mater.* **34**, [10.1002/adma.202107779](https://doi.org/10.1002/adma.202107779) (2022).
- [19] X. Chen, H. Wang, H. Liu, C. Wang, G. Wei, C. Fang, H. Wang, C. Geng, S. Liu, P. Li, H. Yu, W. Zhao, J. Miao, Y. Li, L. Wang, T. Nie, J. Zhao, and X. Wu, Generation and control of terahertz spin currents in topology-induced 2d ferromagnetic $\text{Fe}_3\text{GeTe}_2/\text{Bi}_2\text{Te}_3$ heterostructures, *Adv. Mater.* **34**, [10.1002/adma.202106172](https://doi.org/10.1002/adma.202106172) (2022).
- [20] A. Milosavljević, A. Šolajić, S. Djurdjović Mijin, J. Pešić, B. Višić, Y. Liu, C. Petrovic, N. Lazarević, and Z. V. Popović, Lattice dynamics and phase transitions in $\text{Fe}_{3-x}\text{GeTe}_2$, *Phys. Rev. B* **99**, 214304 (2019).
- [21] A. F. May, S. Calder, C. Cantoni, H. Cao, and M. A. McGuire, Magnetic structure and phase stability of the van der waals bonded ferromagnet $\text{Fe}_{3-x}\text{GeTe}_2$, *Phys. Rev. B* **93**, 014411 (2016).
- [22] V. Y. Verchenko, A. A. Tsirlin, A. V. Sobolev, I. A. Presniakov, and A. V. Shevelkov, Ferromagnetic order, strong magnetocrystalline anisotropy, and magnetocaloric effect in the layered telluride $\text{Fe}_{(3-\delta)}\text{GeTe}_2$, *Inorg. Chem.* **54**, 8598 (2015).
- [23] J.-X. Zhu, M. Janoschek, D. S. Chaves, J. C. Cezar, T. Durakiewicz, F. Ronning, Y. Sassa, M. Mansson, B. L. Scott, N. Wakeham, E. D. Bauer, and J. D. Thompson, Electronic correlation and magnetism in the ferromagnetic metal Fe_3GeTe_2 , *Phys. Rev. B* **93**, 144404 (2016).
- [24] N. León-Brito, E. D. Bauer, F. Ronning, J. D. Thompson, and R. Movshovich, Magnetic microstructure and magnetic properties of uniaxial itinerant ferromagnet Fe_3GeTe_2 , *J. Appl. Phys.* **120**, 083903 (2016), <https://doi.org/10.1063/1.4961592>.
- [25] S. Chikazumi, *Physics of Ferromagnetism* (Oxford University Press, 1997).
- [26] J. Rodríguez-Carvajal, Recent advances in magnetic structure determination by neutron powder diffraction, *Physica B: Condens. Matter* **192**, 55 (1993).
- [27] R. Reisser, R. K. Kremer, and A. Simon, Magnetic phase-transition in the metal-rich rare-earth carbide halides Gd_2XC ($X = \text{BR, I}$), *Physical Review B* **52**, 3546 (1995).
- [28] R. Reiser, R. K. Kremer, and A. Simon, 3d-xy critical-behavior of the layered metal-rich halides gd_2fe_2 , Gd_2ICo_2 and Gd_2BrFe_2 , *Physica B* **204**, 265 (1995).
- [29] Y. Liu, V. N. Ivanovski, and C. Petrovic, Critical behavior of the van derwaals bonded ferromagnet $\text{Fe}_{2.72}\text{GeTe}_2$, *Physical Review B* **96**, [10.1103/PhysRevB.96.144429](https://doi.org/10.1103/PhysRevB.96.144429) (2017).
- [30] B. Liu, Y. Zou, S. Zhou, L. Zhang, Z. Wang, H. Li, Z. Qu, and Y. Zhang, Critical behavior of the van der waals bonded high T_C ferromagnet $\text{Fe}_{2.72}\text{GeTe}_2$, *Scientific Reports* **7**, [10.1038/s41598-017-06671-5](https://doi.org/10.1038/s41598-017-06671-5) (2017).
- [31] Y. S. Touloukian, R. K. Kirby, E. R. Taylor, and T. Y. R. Lee, *Thermophysical Properties of Matter - the TPRC Data Series. Volume 13. Thermal Expansion - Nonmetallic Solids* (John Wiley and Sons Ltd, 1977).
- [32] R. C. Tolman, *The Principles of Statistical Mechanics* (Oxford University Press, Oxford, 1938).
- [33] D. Kim, C. Lee, B. G. Jang, K. Kim, and J. H. Shim, Drastic change of magnetic anisotropy in Fe_3GeTe_2 and Fe_4GeTe_2 monolayers under electric field studied by density functional theory, *Scientific Reports* **11**, 11567 (2021), pMID: 35442017, <https://doi.org/10.1021/acsnano.1c09150>.
- [34] N.-T. Dang, D. P. Kozlenko, O. N. Lis, S. E. Kichanov, Y. V. Lukin, N. O. Golosova, B. N. Savenko, D.-L. Duong, T.-L. Phan, T.-A. Tran, and M.-H. Phan, High pressure-driven magnetic disorder and structural transformation in Fe_3GeTe_2 : Emergence of a magnetic quantum critical point, *Adv. Sci.* , 2206842 (2023), <https://onlinelibrary.wiley.com/doi/pdf/10.1002/advs.202206842>.
- [35] D. J. O'Hara, Z. E. Brubaker, R. L. Stillwell, E. F. O'Bannon, A. A. Baker, D. Weber, L. B. B. Aji, J. E. Goldberger, R. K. Kawakami, R. J. Zieve, J. R. Jeffries, and S. K. McCall, Suppression of magnetic ordering in Fe-deficient $\text{Fe}_{3-x}\text{GeTe}_2$ from application of pressure, *Phys. Rev. B* **102**, 054405 (2020).
- [36] L. J. De Jongh and A. R. Miedema, Experiments on simple magnetic model systems, *Adv. Phys.* **50**, 947 (2001), <https://doi.org/10.1080/00018730110101412>.
- [37] S. Bao, W. Wang, Y. Shanguan, Z. Cai, Z.-Y. Dong, Z. Huang, W. Si, Z. Ma, R. Kajimoto, K. Ikeuchi, S.-i. Yano, S.-L. Yu, X. Wan, J.-X. Li, and J. Wen, Neutron spectroscopy evidence on the dual nature of magnetic excitations in a van der waals metallic ferromagnet $\text{Fe}_{2.72}\text{GeTe}_2$, *Phys. Rev. X* **12**, 011022 (2022).
- [38] I. Grosu and M. Crisan, Ferromagnetic order in two-dimensional spin systems with dipolar interaction, *J. Supercond. Nov. Magn.* **33**, 1073 (2020).